Geospatial distribution of hydrogen demand and refueling infrastructure for long-haul trucks in Europe

Citation for the original published paper (version of record):
Löfving, J., Brynolf, S., Grahn, M. (2025). Geospatial distribution of hydrogen demand and refueling infrastructure for long-haul trucks in
Europe. International Journal of Hydrogen Energy, 128: 544-558.
http://dx.doi.org/10.1016/j.ijhydene.2025.04.257

(article starts on next page)

International Journal of Hydrogen Energy 128 (2025) 544–558

Contents lists available at ScienceDirect

International Journal of Hydrogen Energy

journal homepage: www.elsevier.com/locate/he

Geospatial distribution of hydrogen demand and refueling infrastructure for long-haul trucks in Europe

Joel Löfving [a,b,*], Selma Brynolf [a,b], Maria Grahn [a,b]

[a] Chalmers University of Technology, TechForH2 Excellence Center, Hörsalsvägen 7A, 412 96, Gothenburg, Sweden

[b] Department of Mechanics and Maritime Sciences, Chalmers University of Technology, Hörsalsvägen 7A, 412 96, Gothenburg, Sweden

ARTICLE INFO

Keywords:
Hydrogen demand
Heavy duty
Topography
Geography
AFIR
GIS
EU policy

ABSTRACT

Using hydrogen as a fuel is one option to reduce impact on climate and environment from heavy-duty road transportation. However, the deployment of a hydrogen refueling network is a major bottleneck. To facilitate this development, it is crucial to better understand appropriate location and sizing of hydrogen refueling stations (HRS). We present a bottom-up, geographically detailed model for simulating energy demand from long-haul hydrogen trucks and determining locations and sizes of HRSs, across all of Europe under different scenarios in 2050. The model, called SVENG, calculates weighted energy demand for network links, considering specific local conditions on each link along the route. These are used by a search algorithm for distributing demand along individual routes and simulate HRS locations and sizes. The model scales linearly, supporting large networks; for this study using 0.6 million rows of origin-destination cargo flow data on a network of 17,000 nodes. We show that the model's novel functionality for calculating dynamic vehicle power requirements has a large impact on the distribution of fuel demand and required refueling infrastructure. Results are compared to the Alternative Fuels Infrastructure Regulation (AFIR) for 2030, showing that this legislation might require more HRS than necessary even in 2050 in some countries, unless vehicle sales increase rapidly. Other countries may need to deploy more capacity by 2050 even at lower rates of adoption.

1. Introduction

The EU has adopted targets requiring truck fleets to decrease their CO_2 emissions, to mitigate the adverse effects on climate and environment from heavy duty transportation [1]. Compared to 2019, new trucks need to, on average, emit 45 % less by 2030, and 90 % less by 2040. This warrants new technical solutions beyond only increasing the efficiency of freight operations. New vehicles running on low emission fuels are needed.

Hydrogen is proposed as a fuel for the next generation of heavy-duty trucks [2,3]. It can be produced using renewable electricity and water [4], and it only emits water vapor when used to convert energy in a fuel cell [5]. Hydrogen trucks could provide long range at low vehicle weight, with short refueling times [6], and are thus of particular interest for long-haul missions [7,8].

Still, there are few hydrogen trucks on the roads. Lack of supporting infrastructure, like refueling stations and distribution systems, is a main barrier to their diffusion [6,9–14], and the deployment of infrastructure needs to start a few years before vehicles can be expected to enter the market [15]. The uncertainty of future fuel demand distribution poses an obstacle for investors [16,17], and needs further assessments to facilitate planning of refueling infrastructure [8,18].

To facilitate hydrogen truck diffusion, the EU has passed the Alternative Fuels Infrastructure Regulation (AFIR) [19]. It requires that hydrogen refueling stations (HRSs) be built along the TEN-T core road network in Europe with a maximum of 200 km distance, and close to urban centers, by 2030 [20]. While AFIR enables initial market entry of hydrogen trucks, these might not constitute a significant market share of the total transport work in Europe until further into the future [21]. Better understanding the demands of a future, larger hydrogen truck fleet is important, to evaluate AFIR, and plan how the refueling network needs to develop further.

Refueling demand data with high geospatial resolution and large geospatial scope could improve this planning [22,23], but it is currently lacking [24]. Spatial characteristics, like road speed and slope, are furthermore important when determining the energy consumption of a vehicle [25,26], especially considering the high weight of trucks. This has been omitted in previous large-scale assessments, and could

* Corresponding author. Chalmers University of Technology, TechForH2 excellence center, Hörsalsvägen 7A, 412 96, Gothenburg, Sweden.
E-mail addresses: joel.lofving@chalmers.se (J. Löfving), selma.brynolf@chalmers.se (S. Brynolf), maria.grahn@chalmers.se (M. Grahn).

https://doi.org/10.1016/j.ijhydene.2025.04.257
Received 14 November 2024; Received in revised form 20 March 2025; Accepted 14 April 2025
Available online 18 April 2025

potentially impact the fuel demand distribution. To represent a large fleet, a large number of distinct international flows need to be represented, which is often not the case in the existing literature.

To address these gaps in our current knowledge, the aim of this article is to.

- Present a model that incorporates high geospatial detail, specific vehicle power requirements, and a large number of flows, for simulating fuel demand distribution for a sizeable long-haul hydrogen truck fleet across Europe in 2050.
- Analyze the requirements on a hydrogen refueling station network throughout Europe in 2050, contrasting it with AFIR, and sharing the underlying data for further assessments.

1.1. Previous studies addressing geospatial demand of alternative fuels

Several models have been developed to deal with sizing and location of alternative refueling stations. Urban- or country level models are common, but there are few international models studying hydrogen refueling station location [27]. Country level models are often based on mathematical optimization algorithms (linear/integer/binary etc.), covering the largest amount of transportation flow possible with a given number of refueling stations [16,28–36]. In these studies, it is common to use logistics- or travel data on the origin-destination (OD)-pairs format, which represent goods- or passenger flows between two points or regions along a road network. As an example, Hodgson [29] proposes a flow capturing location model that has later been adapted to distribute a certain number of refueling stations/charging points to maximize covered flow for passenger cars [30–32]. A similar approach is used for heavy-duty hydrogen vehicles in Germany and Italy, by Rose et al. [33] and De Padova et al. [34] respectively, optimizing for cost. Liu et al. [35] builds on the same framework, optimizing for demand cover across the US. Fulton et al. [16] also uses an optimization algorithm (further described by Acharya et al. [36]) for distributing HRSs to different regions in California, covering many types of hydrogen-fueled vehicles.

Models based on mathematical optimization can be difficult to scale, even though progress has been made to decrease the level of complexity [30]. By limiting the amount of logistics data and the size of the road network, many routes and international flows are often left out, resulting in a trade-off with detail. These limitations are seen in both Rose et al. [33], De Padova et al. [34], and Liu et al. [35]. Still, these studies do give an interesting perspective on how to best locate the first hydrogen stations, since they investigate how to maximize utility from as few stations as possible, as discussed by Reuter-Oppermann et al. [37]. However, with higher levels of technology diffusion there is a need for models that investigate refueling needs in a future transportation system where hydrogen trucks are widely used for large geographical areas, considering many different cargo flows.

Some other studies optimize HRS locations without considering vehicle flow, on country [38–40] or more commonly on urban/single highway [41–45] level. Demand is determined by extrapolating average regional transport activity, fuel sales, or similar, and converting the energy demand to hydrogen. This might be reasonable when studying hydrogen cars, typically operating in a confined area. For long distance trucks, however, this would misrepresent the movement pattern of vehicles. It would also disregard the impact on operations by technical parameters like efficiency and tank size, which may affect refueling behavior.

Other, non-optimizing, modeling approaches have been used to address the location and sizing of refueling stations, successfully including more flow data. Speth et al. [28] ditribute charging stations for battery electric trucks at even intervals across Germany and use flow data to calculate their sizing needs. While less complex and thus faster to run, this simplification could result in more stations than necessary [37]. Assuming drivers will charge their battery electric trucks where they need to stop for rests and shorter breaks, Shoman et al. [46] uses OD-data (based on Speth et al. [47]) to find the number of charging points that could be expected in regions across Europe. This procedure manages to include a large number of international flows. However, the underlying assumption of fueling strictly on breaks does not apply to hydrogen vehicles, since their refueling times are expected to be similar to that of diesel [48].

None of the above studies attempt to compute specific vehicle power requirements based on local conditions, even though factors like speed and inclination have a notable impact on required energy. A flat average energy use factor is generally used, but the reason for choosing it is often opaque. Vehicle power requirements have been included when studying energy demand distribution for hydrogen trucks running on single routes in Pihlatie et al. [49] and to some extent in Danebergs [50]. Çabukoglu et al. [7] included vehicle power requirements when studying the Swiss truck fleet, but modeled each vehicle using the same driving cycle. To our knowledge, vehicle power requirements have not been incorporated previously when modeling energy demand for multiple different routes simultaneously in a refueling infrastructure assessment.

1.2. Model contribution

The model developed for this study is an energy demand distribution simulation, combining three main algorithms for (1) calculating dynamic route energy use, (2) distributing refueling load, and (3) simulating locations for refueling stations. It uses a bottom-up approach, employing a series of novel algorithms drawing on fine-grained logistics data, on a road network with high geospatial resolution. It is called SVENG (Simulating Vehicle Energy Needs Geospatially), and it addresses gaps in previous modeling studies as it.

- Considers all of Europe, including a large network of 17,000 nodes and about 0.6 million routes.
- Incorporates geospatially specific vehicle power requirements, and thus energy demand, depending on road conditions like speed and inclination.
- Includes new algorithms for distributing the refueling load from vehicles, and simulating locations and sizing of refueling stations.

This modeling approach has several benefits. We show that international logistics make up a large portion of total refueling demand from long-haul trucks, which thus far has been missing in many similar studies. We also show that dynamic vehicle power demand has a large impact on the geospatial distribution of simulated infrastructure. The model scales linearly and can accommodate more data than used here.

The dataset provided along with this article consists of projected future geographical locations and sizes of HRSs, across all of Europe. This has not been available previously, and can be used for infrastructure planning or further studies of the viability of different options for the hydrogen supply chain. The dataset is analyzed in this paper to address effects on total hydrogen demand in different countries, refueling station network density, and demand from logistics on-route. We also use the data to provide perspectives on the needed additional hydrogen refueling capacity in 2050, compared to the AFIR mandate in 2030. The simulation is run with different model settings, varying the vehicle average tank size and hydrogen vehicle diffusion. The model is used for hydrogen fuel cell-electric trucks in this study, but it can be adapted to other vehicles and/or drivetrains as well.

2. Methodology

To model the geospatial distribution of hydrogen demand for long-haul trucks around Europe, we follow the procedure shown in Fig. 1. To summarize, correlation factors between historical data for GDP and transport work are used to compute country specific goods flow growth

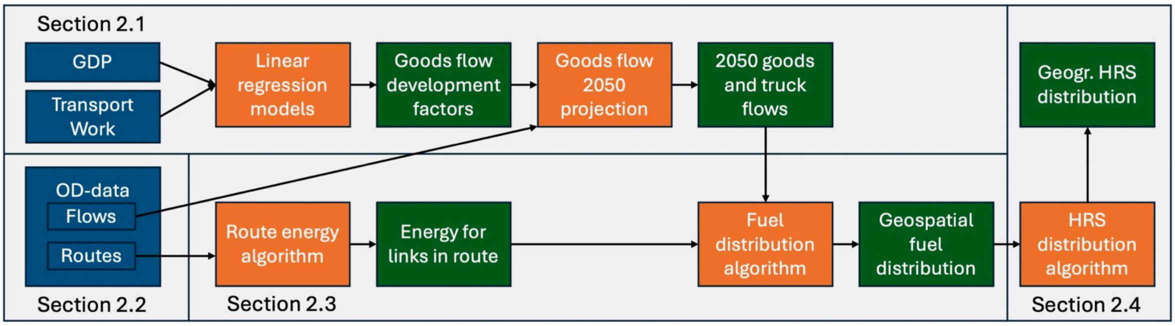

Fig. 1. High level visualization of the model of geospatial distribution of hydrogen demand in European long-distance road freight. Blue boxes represent databases, orange boxes represent algorithms and data management processes, green boxes represent produced datasets. Grey boxes indicate in which section each part of the model is discussed. (For interpretation of the references to colour in this figure legend, the reader is referred to the Web version of this article.)

factors. These are applied to the cargo flows in an OD-dataset, estimating flows between NUTS3 regions (the smallest statistical region level used by the EU [51]) in 2050. In parallel, the energy demand for a single truck traversing each route is computed. This is fed into a fuel distribution algorithm, allocating fuel along the route based on number of trucks, their technical specifications, and trip energy demand. When this is done for all routes, locations for discrete HRSs are simulated to meet demand. Since hydrogen trucks are primarily expected to be interesting for long-haul freight, the freight traffic *within* NUTS3-regions is not considered in this study. This is similar to De Padova et al. [34] studying hydrogen trucks, and Shoman et al. [46] studying battery electric trucks.

In the base case, we assume that 15 % of the long-range trucks on European roads are running on hydrogen in 2050 (with the same share for each of the different cargo flows). This assumption follows work done by Tarvydas [52], where eight reports on scenarios for hydrogen in the total transportation sector are compared. Based on the variation in these findings, the model is also run with different levels of hydrogen technology diffusion between 5 and 35 % for some additional analyses.

2.1. Building modules for country specific cargo flow growth

Linear regression was used for projecting future transport work development for each country individually. Each country's GDP_{PPP} from the World Bank [53] was correlated with national and international cargo tonnage respectively. We represent cargo flow within a country, using an approach similar to Speth et al. [47], by summing national transport tonnage [54] with cabotage [55]. International outgoing figures [56] were used for the international tonnage. Annual data from the period 2010–2019 was used. The correlation factors from the linear regression model were applied to future GDP projections from the Shared Socioeconomic Pathway "Middle of the road" scenario (commonly called SSP2) [57,58]. The produced growth factors for each country between the base year 2010 (which is the base year for the OD-data described in section 2.2) and future year 2050, for national and international cargo flows, can be found in tables A1 and B1 in appendices A and B, respectively. These are accompanied by model coefficients, and with R^2 and F-statistic values to describe model fitness for each country.

2.2. OD-data for long-haul trucks

Like Speth et al. [47], we used data from ETISplus [59] to determine cargo flow tonnage between NUTS3-regions [51] in year 2050. For each OD-pair, we multiply the cargo flow tonnage with a growth factor based on the country of origin, using the national- or international one depending on the destination country. The number of trucks going between an OD-pair is then calculated by dividing the cargo tonnage in year 2050 with the EU average payload for long-haul trucks. The average payload for laden trucks is 13.8 tons [60], and to account for the approximately 20 % empty trucks in Europe [61] (similarly to Speth et al. [47]), we divide this average by 1.25 and assume an average payload of 11.04 tons.

To restrict our analysis to only include long-haul trucking operations, we have excluded all OD-pairs where the total distance of the route is < 360 km, based on discussion by Shoman et al. [46]. We also exclude all routes where the projected annual transport demand in 2050 is less than the equivalent of 10 trucks annually, which removes 33 % of the routes with 1.2 % of the total annual transport work (in tonnes*km, tkm) for long-haul operations. This leaves us with just over 597,000 OD-pairs, running on a network with more than 17,000 nodes as shown in Fig. 2. It should be noted that this network is not identical to TEN-T, but rather somewhat more comprehensive. Flows to and from Russia, Morocco and Turkey are included in the dataset – these are included in the analysis, but the countries are left out of the assessment of hydrogen demand distribution since they are likely subject to more flows from

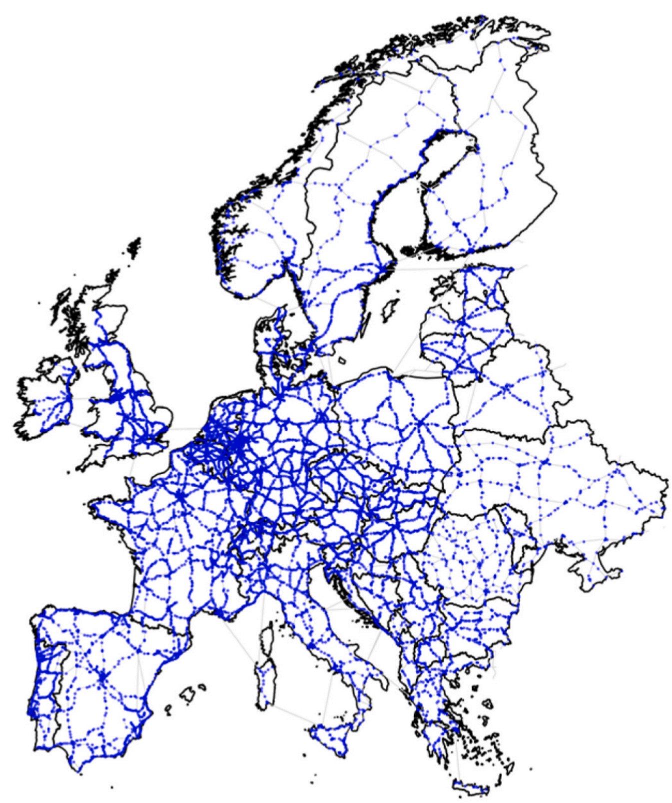

Fig. 2. The modeled road network, with blue dots representing the nodes and grey lines their connections. (For interpretation of the references to colour in this figure legend, the reader is referred to the Web version of this article.)

other regions not present in the dataset. Iceland and Cyprus are not included in the assessment, since they don't have any road network included in the dataset.

2.3. Energy distribution module – dynamic power algorithm

The Dynamic Power algorithm developed in this paper is run in four steps: (1) calculate the power needed on the different links in a route, (2) calculate the energy needed on the different links in a route, and thus the total energy, (3) distribute on-route refueling of trucks on the route and (4) distribute arrival refueling (the portion of the tank that is empty when arriving). For comparison, a simpler algorithm is used, called Constant Power algorithm which is briefly explained in section 2.5.

We assume that all trucks start with a full tank in their origin region, and refuel close to where they are likely to have depleted 80 % of their tanks. Technical details are given in section 2.3.2. Since multiple trucks traverse the same route, and all of them won't stop to refuel in the exact same place, we assume that they will stop for refueling between 70 and 90 % of their tank capacity. To represent this variation in refueling location, one of the algorithms distributes the refueling load from all trucks on the route using a weighted probability density function (PDF) within this interval, centered on the point where tanks would be depleted to 80 %. This "on-route" refueling is marked orange in Fig. 3, which shows a simplified example of how fuel distribution along a route could appear. Upon arrival the tanks are likely not full, and filling up the remainder of a tank is distributed in a similar manner in the nodes close to the point of arrival, marked in purple in Fig. 3. This is also important for our assumption that the trucks start their routes with a full tank.

2.3.1. Routes

To tie the cargo flows to specific roads, Speth et al. [47] have routed each OD-pair along the shortest available path on the nodes and links making up the highway and related access roads in the road network given in ETISplus [59]. The links include data on distance, which nodes they span, and their speed limit. Additionally, we have overlayed the road network with topographical data [62] in a geographical information system (GIS), giving the elevation for each node in the road network. The average inclination for each link can then be calculated using its distance and start- and end elevation.

Since the OD-data is given between NUTS3 regions, Speth et al. [47] optimized the routes between the nodes closest to the centers of the two regions. The distance from this node to the center point was then added to both ends of the route. We have assumed that the inclination for this added distance is 0, for simplicity, and that the road speed is 60 km/h to represent driving on smaller roads for the first and last part of the route [63].

2.3.2. Calculating the power needed for each link

For each route, the power "at the wheels" is calculated for each link (P_{link}, in kW). This is done using the standard vehicle power equations, where P_{roll}, P_{air}, and P_{incl} represents added power requirements due to rolling resistance, air resistance, and inclination respectively [64,65]:

$$P_{link} = P_{roll} + P_{air} + P_{incl} \qquad \text{Eq. 1}$$

where

$$P_{roll} = C_{roll} \cdot (m_{truck} + m_{cargo}) \cdot g \cdot v \cdot \cos \Theta \qquad \text{Eq. 2}$$

$$P_{air} = \frac{1}{2} \cdot \rho \cdot A \cdot C_D \cdot v^3 \qquad \text{Eq. 3}$$

$$P_{incl} = (m_{truck} + m_{cargo}) \cdot g \cdot v \cdot \sin \Theta \qquad \text{Eq. 4}$$

The variables v and Θ here denote the velocity (in m/s) and the inclination (in degrees), respectively. The other constants included in the calculation are described in Table 1.

Regenerative braking is considered when going downhill, in cases where P_{link} becomes negative. This is explained further below. The acceleration force P_{acc}, and associated regenerative braking, are not included in the model. This is due to a large variation between individual driving styles [63]. Ambient weather conditions also affect system efficiency, through need for increased cooling or heating of battery and fuel cell [67], or through varying drag or rolling resistance in windy or wet weather. This is not considered in the model. For links representing ferry lines, the power is set to 0 kW.

Generally, the maximum allowed speed for heavy duty trucks on highways in Europe is 80 km/h [68]. However, it is often assumed that trucks are cruising at somewhat higher speeds on large roads [63,65], and we assume that trucks on any road link with a speed limit above 80 km/h will run at 85 km/h.

The technical specifics of the fuel cell truck are given in Table 2. We assume that the fuel cell has a rated power P_{FC_max} of 300 kW. Fuel cell trucks also have a battery for balancing power needs, which we assume to have a power P_{bat_max} of 400 kW [69]. On some links the power requirement to travel at the speed limit becomes higher than these two

Table 1
Constants included in vehicle power equation.

Name	Value	Description	Source
C_{roll}	0.0055	Rolling friction coefficient	[65]
m_{truck}	14,400 kg	Tractor + trailer empty weight	[65]
m_{cargo}	11,040 kg	Cargo weight	[60]
g	9.80665 m/s^2	Standard gravity acceleration	
ρ	1.2 kg/m^3	Air density, ambient temperature	[66]
A	10 m^2	Long-haul truck frontal area	[65]
C_D	0.6	Aerodynamic drag coefficient	[65]

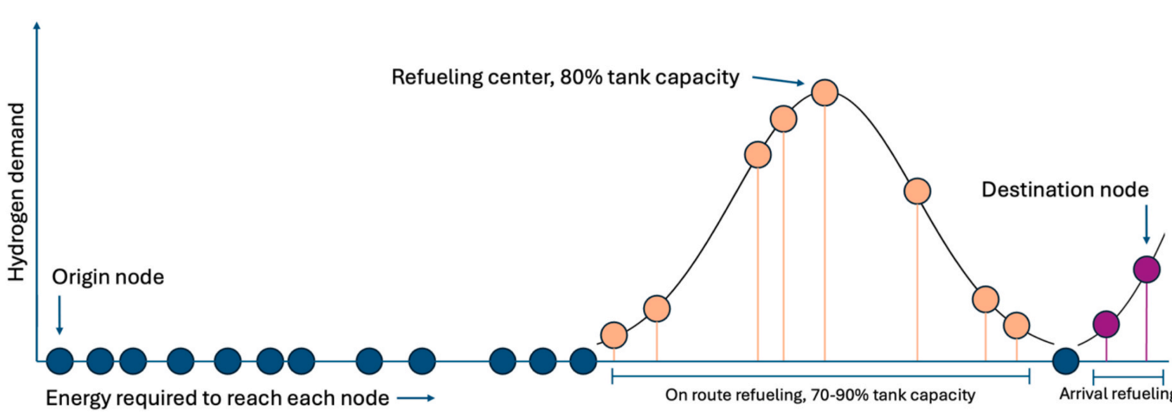

Fig. 3. Example fuel distribution to nodes on a route.

Table 2
Technical characteristics and assumptions for simulated trucks.

	Value	Description	Source
P_{FC_max}	300 kW	Fuel cell rated power	[69]
P_{bat_max}	400 kW	Battery rated power	[69]
Tank pressure	700 bar	Operating pressure for onboard hydrogen tanks	Assumption based on discussion with industry
Tank size (base case)	75 kg	Size of onboard hydrogen tanks	Assumption based on discussion with industry
$\eta_{driveline}$	0.93	Efficiency, drivetrain to wheels	[49]
$\eta_{FC_{high\_load}}$	0.4	Fuel cell efficiency at high loads	[25]
$\eta_{FC_{mid\_load}}$	0.5	Fuel cell efficiency at medium loads	[25]
$\eta_{FC_{low\_load}}$	0.6	Fuel cell efficiency at low loads	[25]
$BOP_{FC_{high\_load}}$	0.9	Factor of remaining power after supplying balance of plant at high loads	[70]
$BOP_{FC_{mid\_load}}$	0.9	Factor of remaining power after supplying balance of plant at medium loads	[70]
$BOP_{FC_{low\_load}}$	0.5	Factor of remaining power after supplying balance of plant at low loads	[70]
C_{idling}	1.02	Factor of additional energy spent on idling on route	[35]
η_{bat_charge}	0.9215	Battery efficiency (including inverter and battery) for charging during regenerative braking	[49]

combined, due to steep ascent. If this happens, the speed on that link is lowered in 5 km/h increments until the power requirement is < 700 kW. This is to represent that a truck might need to slow down to be able to carry itself uphill. Fuel cell and battery are not distinguished in the power calculation since we assume that the battery will ultimately have to be charged by the fuel cell. Fuel cell efficiency (η_{FC}) and balance of plant (BOP_{FC}) energy penalty (for compressors, cooling etc.) are differentiated depending on load, as shown in Table 2. This is defined as high load ($P_{link} \geq 200$ kW), mid load (200 kW $> P_{link} \geq 50$ kW), or low load ($P_{link} < 50$ kW). We also include a factor of 2 %, C_{idling}, to account for energy consumed while idling based on modeled energy cost in Liu et al. [35].

If the load is low enough to require negative power (P_{link} <0 kW), then this power is considered to charge the battery of the truck. This power is not subjected to the same efficiency as the fuel cell, but a higher efficiency representing the battery and inverter (η_{bat_charge}). If the power for charging the battery goes above the rated power of the battery $P_{bat\,max}$, then the speed of the vehicle is lowered on that link in the same manner as for limiting the propulsion power going uphill, until it is below the rated power of the battery. Balance of plant, and battery maximum storage capacity, are not considered when charging the battery.

This whole calculation procedure is performed for each individual route separately. The inclination between all sequential points is computed for each new route, ascertaining that they are considered in the right order and that the inclination is in the right direction.

The tank size is set to 75 kg in the base case. However, depending on technology choices and future R&D, tank sizes might be larger or smaller in general. Basma and Rodríguez [71] suggest the maximum future tank size to be 54 kg for 700 bar tanks, and Ahluwalia et al. [72] simulate the technical performance of liquid hydrogen tanks at close to 90 kg. Tank sizes are thus varied for some model runs, for the assessments presented in sections 3 and 4.

2.3.3. Calculating the energy needed for each link

After calculating the total power P_{link} for each link on the route, the total hydrogen energy E_{link} in kWh for traversing each link can be computed for all links as follows:

$$E_{link} = \frac{P_{link}}{\eta_{ec} \cdot \eta_{driveline}} \cdot \frac{d_{link}}{v_{link}} \cdot C_{idling} \qquad \text{Eq. 5}$$

where d_{link} and v_{link} are expressed in km and km/h, respectively, and d_{link}/v_{link} thus equals the time in hours spent on the link. η_{ec} is the product of η_{FC} and BOP_{FC} (considering different loads) for forward propulsion (P_{link} >0 kW). When the battery is being charged (P_{link} <0 kW), then $\eta_{ec} = \eta_{bat\_charge}$. Different values for η and BOP are given in Table 2.

Now we have a list of the hydrogen energy required to traverse the links, which we will use to determine where it is likely that trucks will refuel, and to distribute refueling load.

2.3.4. Distributing the on-route energy demand

As shown in the example in Fig. 3, on-route refueling is distributed along the area of the route reachable by 70–90 % of the truck tank capacity, around a node close to 80 % of the tank capacity. We will call this center node the "average refueling level node". This is done in four steps, for each route.

1. Finding the average refueling level node of the refueling distribution
2. Finding the nodes to include in the distribution
3. Computing a weighted PDF for distributing the refueling on these nodes
4. Distributing the sum of the trucks refueling onto the nodes based on the weighted PDF

If, during step 1, it is found that the whole route can be traversed without stopping for a refuel, the remainder of steps are skipped, and all the fuel consumed on the route is assumed to be refueled in the destination nodes. This is described in section 2.3.5.

1. Finding the average refueling level node of the refueling distribution:

First, to lower computation time, an approximation for where on the route 80 % of the tank might be depleted is calculated. We get the total energy for the route by summing the energy required to travel each link, and divide it by the tank size times the average refuel level. This gives us a number for how many times on the route a truck will refuel. The integer part of this number is the number of full fills that will occur on-route, and the decimal part indicates the part of a full tank that will be refueled upon arrival. We use this number to calculate how large portion of the trip will be covered by one tank, and name that value $\boldsymbol{r}$. Fig. 4a shows how this number is used to find an approximated average refueling level. r_{arr} denotes the nodes whose fuel demand will be filled on arrival.

However, since the energy requirements for each link are *not* equal, it is not certain that the average refueling level node, the node closest to r, should be used. To check, we sum the energy needed to reach this node from the origin. If it is within 1 % of the average refueling level, it is considered an appropriate node. If it is higher than this, we go to the previous node and repeat the process until we find a suitable node to represent where 80 % of the tank might be depleted, and vice versa, as shown in Fig. 4b. If more than one full tank is needed to traverse a route, then the process is repeated starting from the last average refueling level node.

2. Finding the nodes to include in the distribution:

After finding the average refueling level node, the rest of the nodes to be included in the refueling distribution should be found. These are the

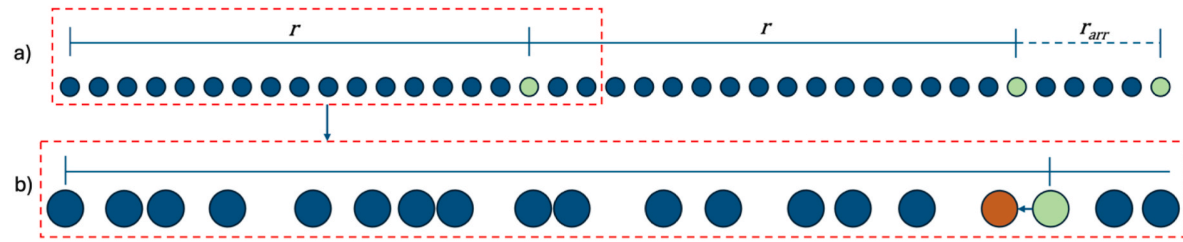

Fig. 4. a) Approximating and b) finding average refueling level nodes along the route. r is the portion of the route covered by 80 % of one tank (refuel level), and r_arr is the portion covered by arrival refueling. Green nodes depict estimated average refueling level nodes, and the orange node in b) depicts a new one being selected when searching for a node in the refueling level interval. (For interpretation of the references to colour in this figure legend, the reader is referred to the Web version of this article.)

other nodes that could be reached with 70–90 % of the tank capacity. For each average refueling level node on the route, we check the nodes before and after it on the routes. For each checked node, the total energy required to traverse the links between it and the average refueling level node is computed and stored in a list $l_{energyweights}$. When the next node requires more than 10 % of the tank capacity to reach, the search is terminated in that direction.

For subsequent on-route refueling events, on long routes, we assume the refueling distribution to become more and more uncertain. The limit to the spread of the refueling event is multiplied by its number in the order, meaning that the second refueling event is spread within 20 % of the tank capacity in each direction of the average refueling level node, and so on. This, conceptually, would represent the truck refueling at 70 % of the tank capacity in the first refueling event to refuel after using 70 % of the tank capacity also the second time.

The nodes that do not get an energy weight in this process get a prohibitively high weight assigned instead. The fuel center gets the weight 0, statistically representing zero-unit distance from the mean of the distribution.

3. Computing a weighted PDF for distributing the refueling on these nodes:

Once the route has a list with node weights $l_{energyweights}$, we run it through the PDF (with σ as the standard deviation) to generate the weighted list:

$$f_{pdf}\left(l_{energyweights}, \sigma\right) = \frac{1}{\sigma\sqrt{2\pi}} e^{-\frac{1}{2}\left(\frac{l_{energyweights}}{\sigma}\right)^2} \quad \text{Eq. 6}$$

This gives us a continuous function for the probability of refueling in a certain node. However, it is only possible to refuel in discrete nodes along the function of probabilities. We, thus, need to compute a list of normalized discrete probabilities by:

$$l_{pdf\_normal} = \frac{f_{pdf}\left(l_{energyweights}, \sigma\right)}{\sum f_{pdf}\left(l_{energyweights}, \sigma\right)} \quad \text{Eq. 7}$$

where l_{pdf_normal} is a list of weights with a total probability equal to 1.

4. Distributing the sum of the trucks refueling onto the nodes based on the weighted PDF:

Once the PDF weights are computed, they are multiplied with the projected number of hydrogen trucks going on the route in 2050 (N_{trucks}) times the average refueling level (C_{refuel_level}) of a the energy content of full tank ($E_{full\_tan\ k}$), by:

$$l_{refuel} = l_{pdf\_normal} \cdot N_{trucks} \cdot E_{full\_tank} \cdot C_{refuel\_level} \quad \text{Eq. 8}$$

2.3.5. Distributing the arrival energy demand

The procedure for allocating arrival fuel demand, marked purple in Fig. 3, is similar to that for on-route demand. The last node on the route is assigned as the average refueling level node, and the other nodes in which drivers are likely to refuel are again considered to be those that could be reached on less than 10 % of the tank capacity from this node. The procedure for finding those nodes and assigning their refueling probability weight is the same as described for on-route refueling.

When calculating arrival refueling, the decimal part of the total number of refuels ($C_{arrival\_fuel}$) on the route is used, as mentioned earlier (see equation (9)). This is to only refuel the remaining portion of the trip, not covered by the previous full tanks. Note that for many routes, this is the only refueling on the entire route.

$$l_{arrival} = l_{pdf\_normal} \cdot N_{trucks} \cdot E_{full\_tank} \cdot C_{arrival\_fuel} \cdot C_{refuel\_level} \quad \text{Eq. 9}$$

2.4. Locating and sizing HRS

After refueling load from all routes have been distributed to nodes, this data is used in an algorithm for locating HRSs. Speth et al. [47] assumes all routes between NUTS3-regions to start and end in the middle of the region. However, this might not necessarily be where most trucks go. As such, HRS are redistributed onto truck fuel stations and rest stops, using an algorithm described in section 2.4.2. Before that, in section 2.4.1, we describe how we processed data for ranking locations for receiving an HRS.

2.4.1. HRS location ranking data

Data provided in Link and Plötz [73] gives the location for over 19, 000 truck stops across Europe. We consider these nodes as the primary candidates for building HRSs. Along with the position, the authors provide some data points for each truck stop; one of which is the highest annual number of passing trucks on any road link within a 5 km radius. We will refer to this data point as the “truck flow count”. Like in this study, that data considers the same road network as used in Szimba et al. [59] and Speth et al. [47], and also uses the modeled truck flows from the latter. The truck flow count is used as the primary means for weighting the distribution of HRSs.

In NUTS3 regions without any truck stops within 5 km from the road network, we weight HRS distribution onto truck stops according to population density. We overlaid the truck stop nodes with population data from the EU census 2021 [74] and UK census 2011 [75]. Both datasets are GIS-compatible and given with a 1 × 1km^2 resolution. Ultimately, this measure is only used in two NUTS3-regions.

In countries not among the EU or UK, we use road nodes as candidates for HRS locations. These are weighted by simulated hydrogen demand.

2.4.2. Algorithm for allocating HRSs

We employ a similar logic to Fuse et al. [76] for allocating HRS. The logic is also related to the one used by Kim et al. [40] for allocating fuel cell vehicles to regions. As visualized in steps 1 and 2 in Fig. 5, the total hydrogen demand in the nodes is summed to first the NUTS3- and then the country level. We then calculate the number of pumps required to

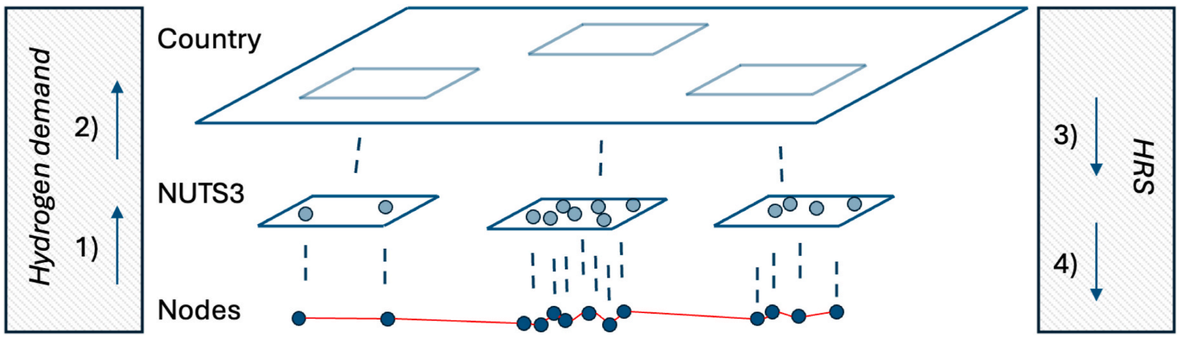

Fig. 5. Visualization of the HRS distribution algorithm. 1) The hydrogen demand from the nodes are summed up to NUTS3 region level, and then 2) to country level. Required number of HRSs per country are calculated, and then distributed 3) to NUTS3 regions and from there 4) to nodes. Red links indicate a road, to give context to the nodes. (For interpretation of the references to colour in this figure legend, the reader is referred to the Web version of this article.)

fulfill the demand for each country. HRSs are considered to be of discrete sizes as defined by Rose et al. [33] based on work by Elgowainy and Reddi [77]. We consider one pump to serve up to 15 trucks per day, 350 days per year. The more pumps allotted to a node, the larger the HRS. HRS sizes are given in Table 3.

After calculating the number of HRS pumps needed in a country, these are distributed onto the NUTS3-regions based on the hydrogen demand in the regions (step 3 in Fig. 5). When the region with the highest level of demand has been allotted a pump, demand equivalent to one pump is deducted from the total demand of that region, and the process is repeated.

With all pumps distributed to the regions, pumps are similarly distributed to suitable nodes (step 4 in Fig. 5). This time it is the node with the highest share of the total truck flow count (or population density/hydrogen demand according to section 2.4.1, where truck flow count is not available) among truck stops in the region that gets the first pump. The inverse of the total number of HRSs for that region is then deducted from the share in this node, before the process is repeated.

In each country, if there is a decimal part of an HRS left, this one is distributed individually; a whole pump is added to the station size but the lower level of demand is registered as a decimal part of a pump in that node.

There is one exception to the above process: the first time a region or a node receives an HRS, nothing is deducted, which means this node or region will also get the next pump if there are any left to distribute. This promotes building stations with two pumps or more, to avoid unreasonably many small HRSs being built very close to each other.

Queueing effects could impact the needed capacity at each station, if many trucks attempt to refuel at the same time. This is not considered in this model.

2.5. Constant power algorithm

To be able to discuss the performance of the Dynamic Power algorithm presented in section 2.3, we also run a Constant Power version of the algorithm. Instead of calculating specific power on each link, this one uses an average energy consumption per km. This average is obtained as the average energy consumption per km between the different routes run in the Dynamic Power algorithm, which is 2.21 kWh/km as depicted in Fig. 7.

Table 3
Hydrogen refueling station (HRS) sizes used in this work, modified from Rose et al. [33] referencing Elgowainy and Reddi [77].

	Unit	XS	S	M	L	XL
Number of trucks	Trucks/day	0–15	15–30	30–60	60–120	120–240
Number of pumps	Pumps	1	2	3–4	5–8	9–16
Daily hydrogen capacity	kg/day	1125	2250	4500	9000	18000
Annual hydrogen capacity	tonnes/year	394	788	1575	3150	6300

2.6. AFIR comparison

As mentioned, the AFIR requires countries to build one HRS every 200 km along the TEN-T core network, and one in every urban node [20]. Using these criteria, the number of refueling stations for each country has been estimated [78]. This data is presented, discussed, and validated in appendix C.

3. Results: model evaluation

To analyze the influence of different features and assumptions on the model, the results from different runs are compared in this section. The Dynamic Power algorithm is compared to the Constant Power algorithm, using the base case tank size of 75 kg. The Dynamic Power algorithm results are also compared for 60 kg, 75 kg, and 90 kg tank sizes, as motivated in section 2.3.2. For these cases, the share of trucks running on hydrogen is 15 %. It is worth mentioning that the Dynamic- and Constant Power algorithms run with similar compute times.

3.1. Route simulation details

To better understand how the model distributes energy, and how different assumptions may affect this, we here present a detailed description of the energy distribution from the Dynamic Power algorithm on one of the 597,000 modeled routes. Fig. 6 shows the results from one route run with a 75 kg tank, between Nordburgenland in Austria and Arrondissement Antwerpen in Belgium. It is 1183 km long and requires 2585 kWh of hydrogen. There are 222 nodes on this trip, running along the x-axis, scaled according to the distance between nodes. The refueling load assigned is indicated by the shaded vertical areas. The speed and elevation are shown as the brown and green lines, respectively, impacting the power requirement (red dashed line) in each link going between the nodes. This in turn affects the cumulative energy demand shown in black. Where the power line is accompanied by a light blue bar, the power required is negative, and the battery is being charged through regenerative braking.

Since the power requirement drives the energy consumption on each link, trucks on some routes will on average spend more or less fuel than they would on an average route. This depends on the link speed and inclination. The route average fuel consumption is used for all routes in the Constant Power algorithm. Compared to the Dynamic Power algorithm, the Constant Power algorithm will thus assign refueling earlier on-route, and more refueling on arrival (or the other way around) for some routes. This results in a shift in assigned refueling infrastructure

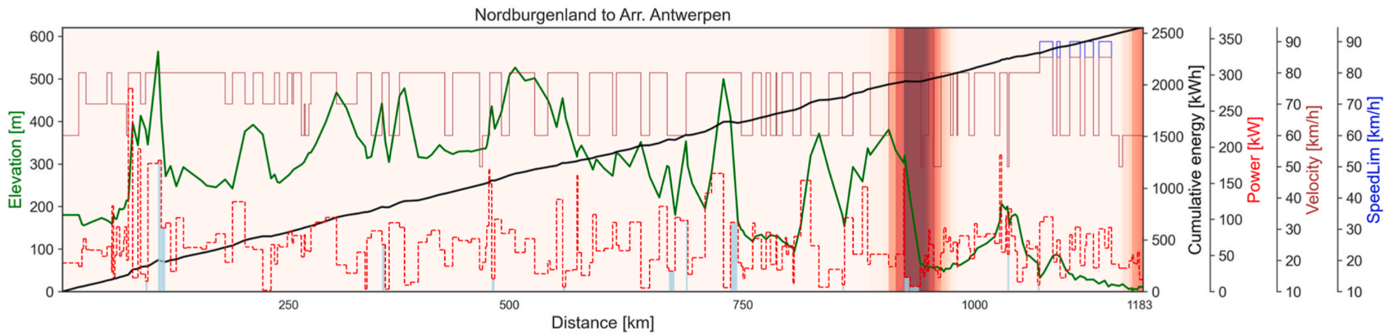

Fig. 6. One simulated route. The x-axis represents distance driven along the route. Elevation (green) and velocity (brown) impacts power (red), which results in a total cumulative fuel demand (black). Where the power is accompanied by a light blue bar, the power needed (P_{link}) is negative and is utilized for regenerative braking, which in turn decreases the cumulative fuel demand. Refueling demand allocated to nodes along the route is depicted with vertical shaded areas. Speed limit (blue) is included to specify where the truck runs slower than the speed limit. (For interpretation of the references to colour in this figure legend, the reader is referred to the Web version of this article.)

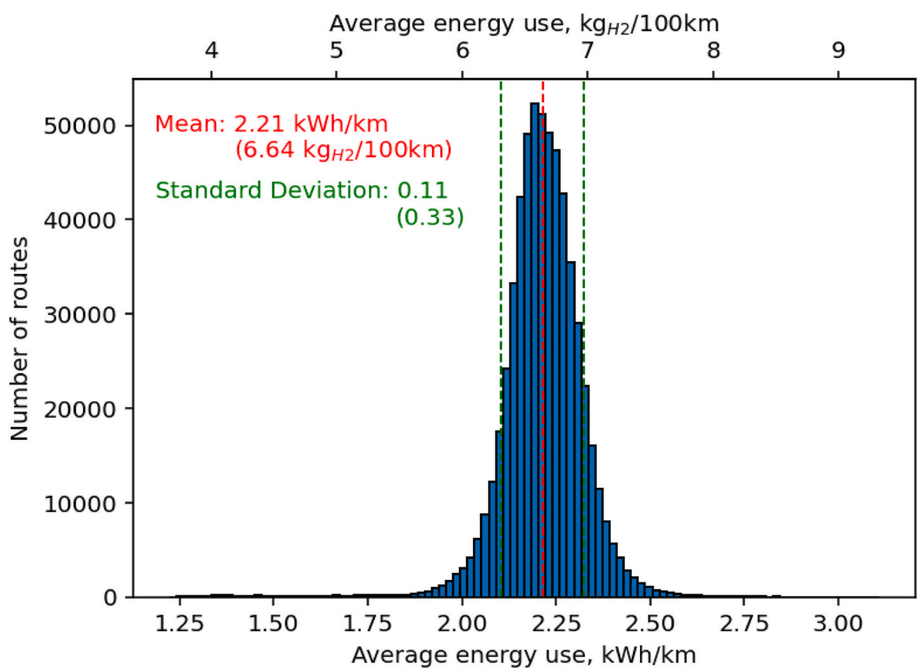

Fig. 7. Distribution of average energy use between the 597,000 routes modeled in this study.

between countries/regions. This is visualized for two routes in appendix D. The total differences between the algorithms are discussed in section 3.3.

3.2. Average energy use per km

After running all routes in the Dynamic Power Algorithm, the average energy per km for each one is calculated. The averages exclude ferry links. The mean of these averages is 2.21 kWh/km with a standard deviation of 0.11, as presented in Fig. 7. This value is used for the Constant Power algorithm. This average is in line with the factor given by Basma and Rodríguez [71] (2.21 kWh/km). The one used by Liu et al. [35] (2.38 kWh/km) is somewhat higher, and outside the standard deviation. Rose et al. [33] (1.63 kWh/km) is considerably lower. For a real-world comparison, a Mercedes Benz truck ran (fully loaded, requiring more energy per km) a 1047 km demonstration run on 88 kg liquid hydrogen [69], which would represent 2.80 kWh/km.[1]

3.3. Model output comparisons

Results from the Dynamic Power base case simulation were compared both with the Constant Power algorithm, as well as with the 60 kg and 90 kg tank Dynamic Power simulations. Fig. 8 displays the differences in the absolute number of HRS pumps for each country in each of the comparisons, and the factor difference in HRS capacity. For the top graph representing the differences between the constant and dynamic algorithms, the most notable countries are Germany and Poland. They receive 229 fewer and 261 more stations, respectively, with the Constant Power algorithm compared to Dynamic Power. For Germany, this decrease corresponds to a third of their capacity, whereas

[1] The average energy consumption in kg_{h2}/100 km would be, for these different sources:2.21 kWh/km = 6.6 kg_{h2}/100 km; 2.38 kWh/km = 7.1 kg_{h2}/100 km; 1.63 kWh/km = 4.9 kg_{h2}/100 km; 2.80 kWh/km = 8.4 kg_{h2}/100 km.

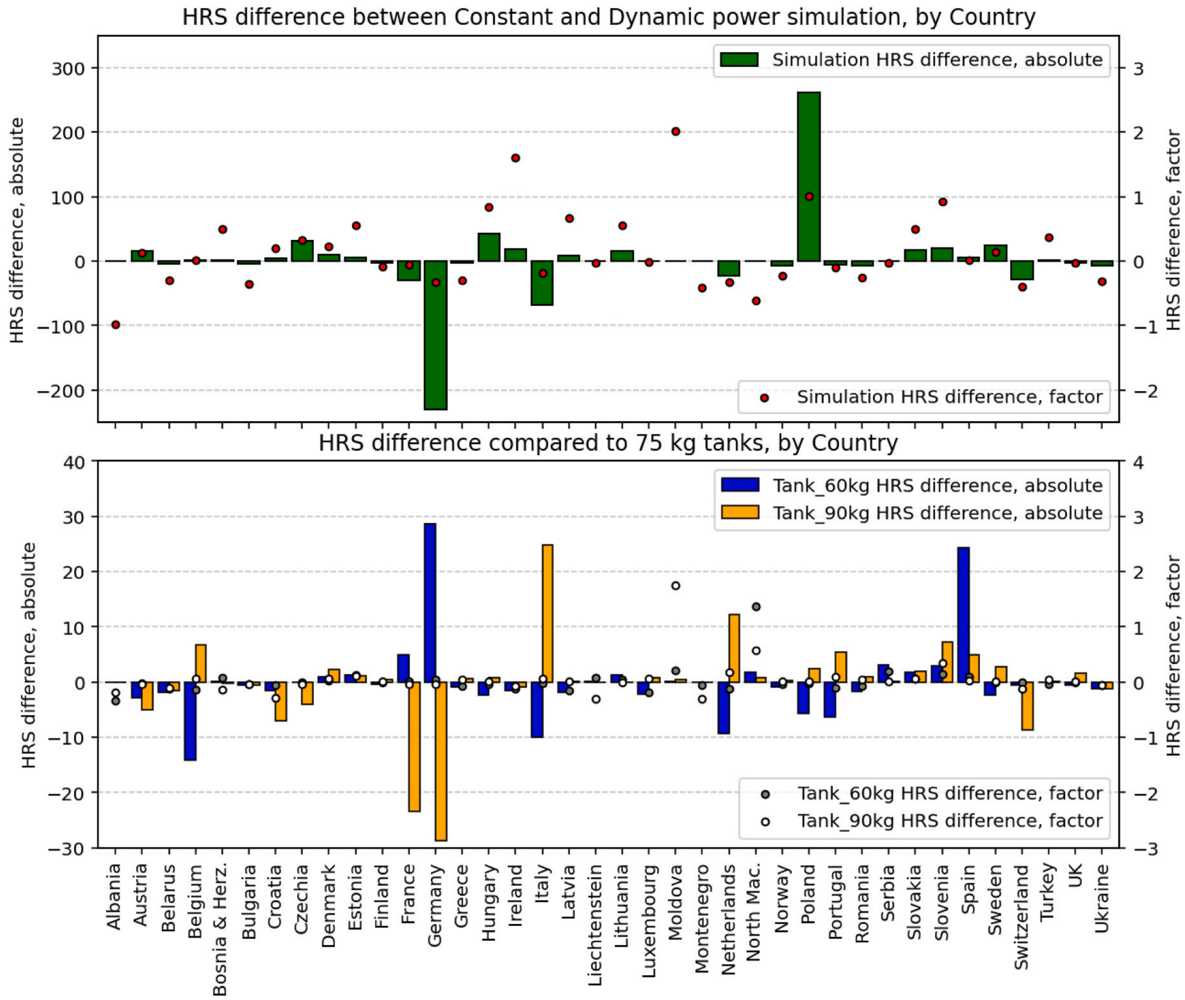

Fig. 8. Differences in number of HRSs for each country individually when comparing the constant and dynamic power algorithms, as well as when assessing the effect of assuming different tank sizes onboard the trucks. The constant power algorithm assumes equal energy consumption on each part of the route, and the dynamic adapts power requirements to local conditions. This is explained in section 2. Note that the y-axes are on different scales.

the increase for Poland means a doubling of the allotted capacity. In the bottom graph, investigating the impact of tank size, the differences are much smaller. The factor change between the scenarios is less than 10 %, except for some countries with very few stations in total. The impact of tank size thus appears marginal compared to the impact of considering dynamic power in this model.

This is also shown on NUTS3 level. When simulating with Constant Power, the number of regions where the difference in HRS pumps is larger than 1 is 449, out of the total considered 1538. When simulating varying tank sizes, the absolute difference is larger than 1 for 192 and 178 regions, respectively. Extreme values vary a lot, and this is elaborated on in appendix D.

4. Results: fuel distribution and AFIR assessment

In this section, we use the simulated datasets to assess the requirements on a future HRS network in Europe. We first present results on the total hydrogen demand and HRS distribution for the base case. Second, we present results on the analyses comparing the simulated HRS network in 2050 to the AFIR rules for 2030. Geospatial HRS data is given, for all simulations using the Dynamic Power algorithm, in appendix G.

4.1. Total hydrogen demand and HRS distribution - base case

The HRS distribution for the base case simulation is shown in Fig. 9. Germany shows the highest total annual hydrogen demand of around 7 TWh annually.[2]

Fig. 10 shows the ratio of refueling load from on-route vehicles compared to arriving vehicles (as defined in section 2.3), for the three modeled tank sizes. On-route refueling contributes to the high total hydrogen demand seen in e.g. Germany and France (see appendix E). Many of the Eastern European countries indicate a low total refueling demand, with a high share of it from passing trucks. Even though we are not comparing these results to fuel demand for shorter range transportation (routes shorter than 360 km, and freight within NUTS3 regions), they point to the importance of including international trade when modeling transportation energy needs and hydrogen infrastructure deployment.

As expected, Fig. 10 also illustrates that the larger the on-board

[2] Annual hydrogen demand, and number of HRSs, on country level can be found in appendix E and F, where results from all runs using the Dynamic Power algorithm are included. HRS distribution on nodes is given as tabulated geographical information as an Excel file, appendix G. Annual hydrogen demand on NUTS3 region level is given in yet another Excel file, appendix H. A third Excel file, appendix I, gives the number of HRS of different sizes for each country and different model run.

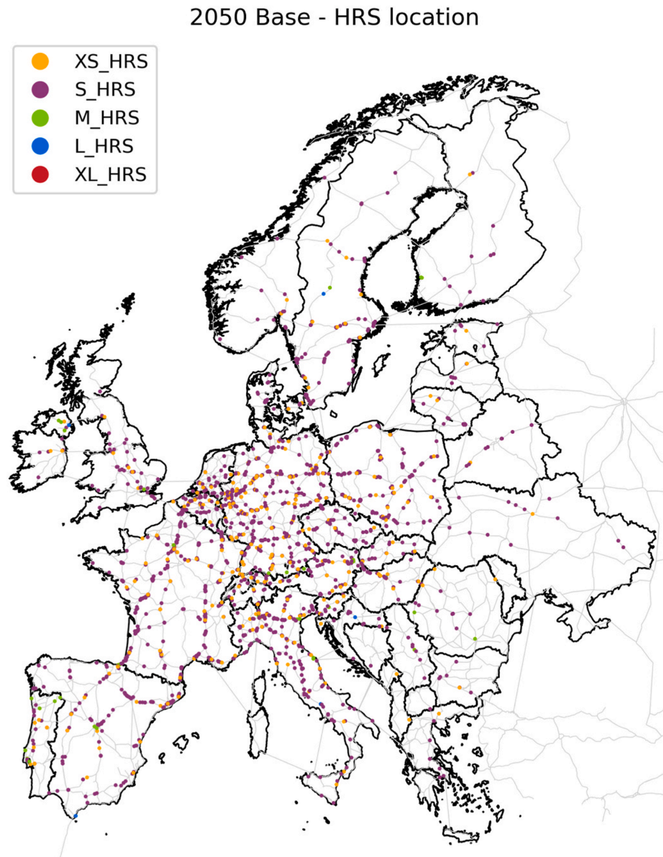

Fig. 9. Simulated location and size of discrete HRS.

hydrogen storage, the more routes can be traversed on one tank. With less refueling needed on-route, more hydrogen infrastructure could be provided close to logistics hubs. This is quantified in Table 4, showing the shares of routes and transport work that can be completed on one tank with the different tank configurations.

4.2. AFIR

The AFIR mandates a certain number of HRS pumps per country by 2030, and each pump needs to be able to supply at least 1000 kg hydrogen per day [20]. Fig. 11 shows the additional capacity required per country by 2050, if 15 % of the long-distance trucks are running on hydrogen using 75 kg tanks. France would need to add more than 7 times the AFIR capacity. On the contrary, Romania, Greece, and Bulgaria have a lower simulated hydrogen demand in 2050, in our base case, compared to the 2030 required supply.

Table 4
Share of routes and tkm, respectively, that can be performed without refueling on-route given the different tank sizes.

Tank size	60 kg	75 kg	90 kg
Routes	27 %	40 %	52 %
Tkm	34 %	45 %	55 %

This relationship also holds when running the Dynamic Power algorithm with 60 kg and 90 kg tanks, or with 75 kg tanks but varying the share of hydrogen trucks between 5 %, 15 %, 25 %, and 35 %. Fig. 12 depicts the added capacity required compared to AFIR for all these cases. If this share is 5 % or less, 9 countries will not make use of their mandated HRS capacity by 2050. However, at this rate most countries would still need equal to or more capacity than AFIR proposes, and at higher adoption rates a significantly larger network would be required than that mandated by the regulation.

In central Europe, the density of modeled HRSs and pumps is the highest, to match the higher demand. This is illustrated in Fig. 13, showing the density of pumps and HRSs, respectively, along the road network considered for this study. Many countries get more than the AFIR mandate on one pump/HRS every 200 km by 2030, but bear in mind that the dataset used in this model includes more road distance than the TEN-T core network, which is the basis of the AFIR legislation.

5. Discussion

The model presented in this article, SVENG, is an attempt to enable new perspectives on the requirements on future hydrogen refueling infrastructure for heavy duty trucks in Europe.

Comparing the results from the Dynamic- and Constant Power algorithms, it is clear that including local road conditions is important in determining where trucks will need to refuel. This especially since hydrogen trucks have a smaller onboard energy storage compared to conventional ones. Failing to include specific truck power requirements would, in this model, result in hundreds of refueling pumps being placed

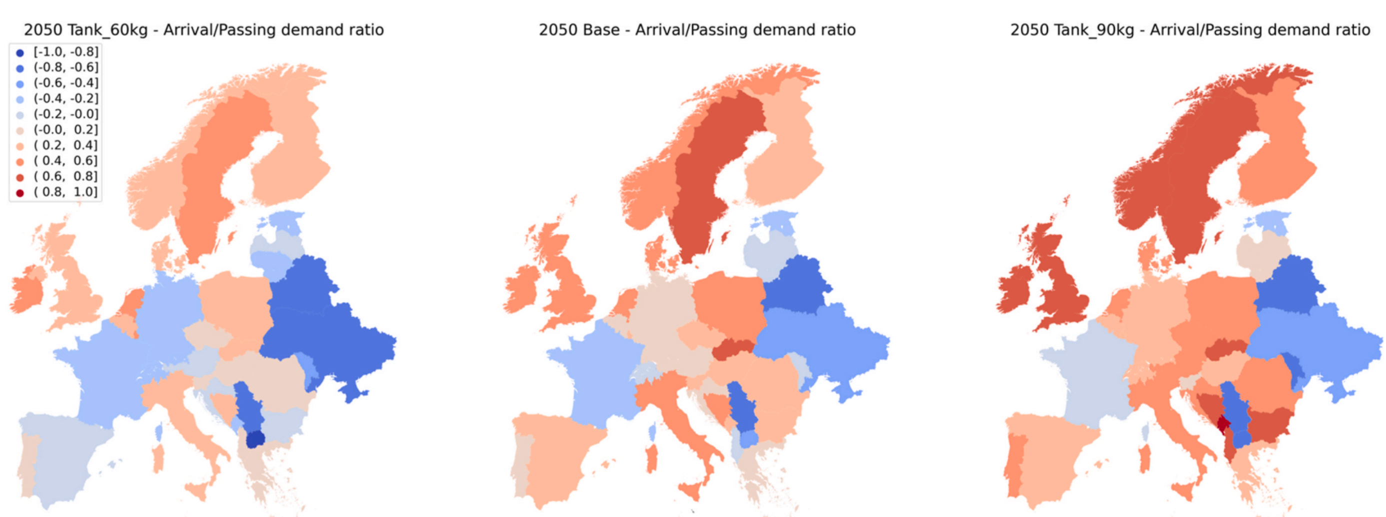

Fig. 10. Model results for different tank sizes, 60 kg (left), 75 kg (middle), and 90 kg (right), comparing the ratio between arrival- and on-route refueling load. −1 (blue) indicates only passing refueling demand, +1 (red) indicates only arrival refueling demand. (For interpretation of the references to colour in this figure legend, the reader is referred to the Web version of this article.)

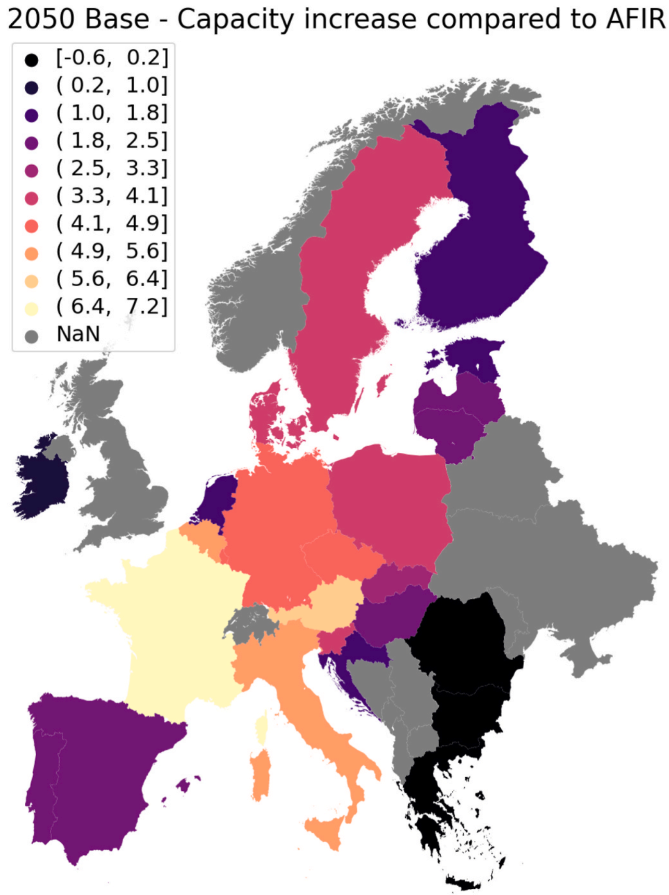

Fig. 11. Additional hydrogen supply needed until 2050, per country, compared to the supply required by AFIR in 2030. Countries with grey Not a Number (NaN) values are not part of the EU and thus not covered by AFIR.

in locations where utilization could be expected to be lower. This indicates that other models would benefit from including a dynamic power perspective, both to increase the level of detail in the assessments, and to further study the impact on dynamic vehicle power across models.

However, there are still many dynamic aspects not covered by this model: varying weather conditions, driver behavior, and notably, different payloads. In some regions, average energy consumption might be higher due to a generally warmer or colder climate, and some regions might see fewer trucks carrying heavier payloads than modeled here. This could impact both the total energy use and the distribution of fueling infrastructure. Beyond energy use on the routes, other factors like logistics planning, fuel prices in different countries, congested traffic situations, and driver preference will all also ultimately affect where refueling is done, which is not represented here. These are all *variable* factors, whereas this study focuses on dynamic adaptation to *static* factors (the inclination and speed limit on a road segment). The former would be interesting to include but are by default hard to capture in simulations on this scale, and it is difficult to estimate their potential impact on the results. The modeling of static factors could also be improved, for example by incorporating road data with higher resolution.

Tank size, and consequently range, is shown to have a smaller influence on where HRSs should be located compared to incorporating dynamic power. However, we do quantify the flexibility associated with increasing tank sizes – with 90 kg tanks instead of 60 kg, the number of long-haul routes that can be traversed without stopping for a refuel doubles. There are many other trade-offs to consider, like technical feasibility and available cargo volume, but this insight could help truck manufacturers and -operators in deciding which solutions to pursue.

Including international logistics is important for determining the total distribution of hydrogen demand from long-haul transportation. This is supported by the relationship between arrival- and on-route refueling presented in the analysis. It can also be discussed by comparing to another large-scale European study done by Rose et al. [33], which includes about 1500 OD-pairs, all representing national flows within Germany. In this article, over 271,000 OD-pairs either start or end in Germany (while others yet are passing through). Rose et al. [33] assume all trucks to run on hydrogen, as opposed to the 15 % used

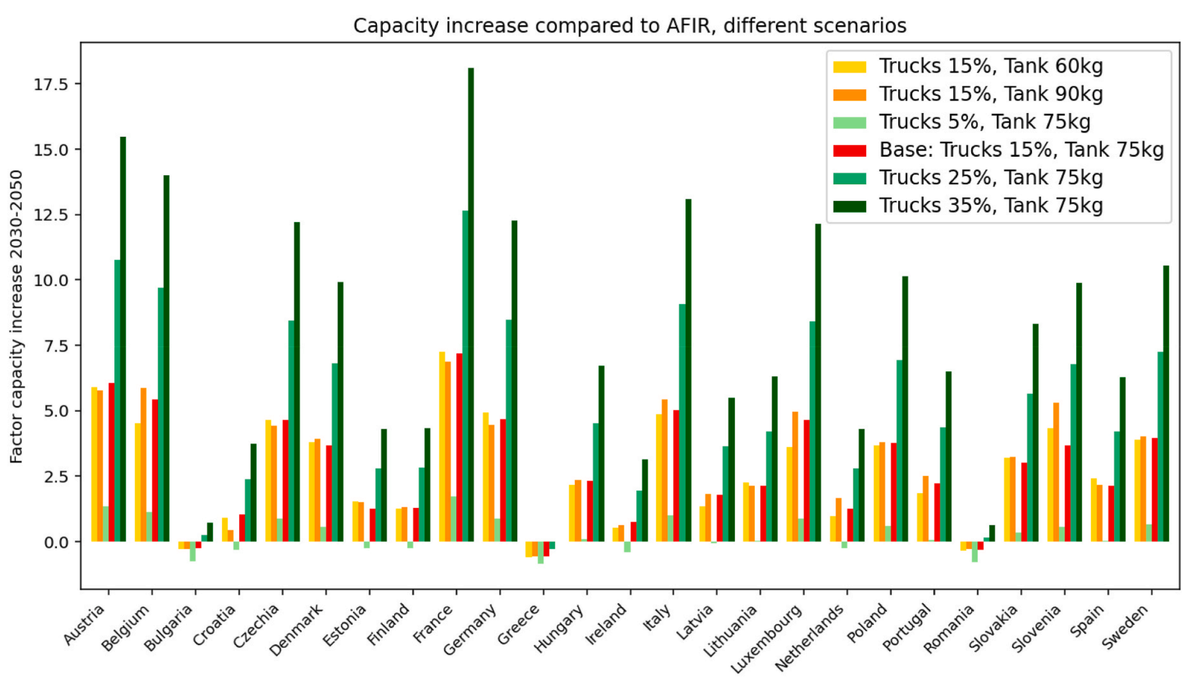

Fig. 12. Multiplicative factor additional hydrogen refueling capacity for long-haul trucks needed until 2050 under the different scenarios, per country, compared to the capacity required by AFIR in 2030.

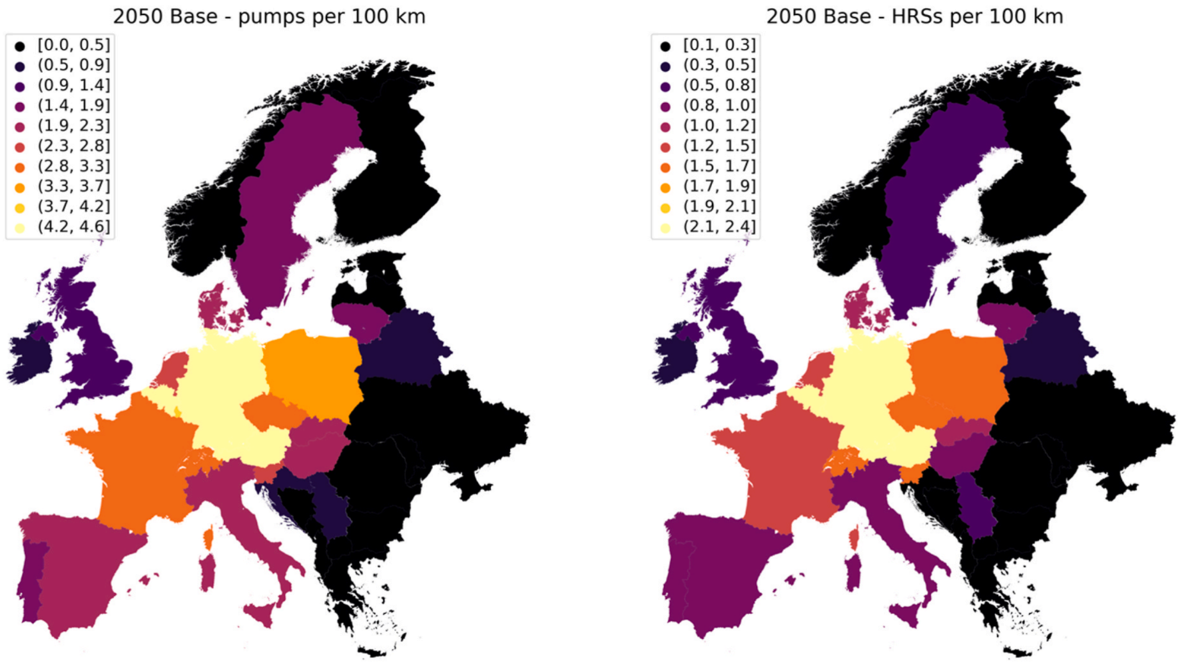

Fig. 13. Number of refueling pumps (left) and discrete HRSs (right) per 100 km, per country. One HRS can hold multiple pumps.

in our base case. The resulting number of discrete HRSs in their study is 142, compared to 382 in Germany seen in this study (as given in appendix F). Although the smaller number of stations has to do with their model being based on optimization, we show that omitting international trade leaves out approximately half of the fuel demand from long-haul trucks in Germany (Fig. 10), which should have a notable impact on this result. Additionally, as mentioned earlier, Rose et al. [33] used a comparatively low, fixed energy use factor. This likely underestimates the total energy use. Furthermore, as shown in section 3.3, the SVENG model underestimated the total number of HRSs in Germany when not considering dynamic truck power requirements. We expect this effect to be present in any study assuming constant energy use.

As indicated above, the choice of modeling framework is another factor that likely has a large influence on the results. By choosing a non-optimizing framework, we have implicitly tasked the model to design the infrastructure according to other principles than comparable studies. As described in section 1.2, the modeling methods used by Rose et al. [33], De Padova et al. [34], Liu et al. [35], and Fulton et al. [16] are all based on optimization. One notable difference is the size and distribution of HRSs; Rose et al. [33], De Padova et al. [34], and Fulton et al. [16] find that their model prioritizes large and few stations, while the model presented here and the one presented by Liu et al. [35] (optimizing for demand cover rather than cost) generally build more and smaller stations. Rose et al. [33] states that the total system utilization in their model goes up if they lower the maximum allowed daily output from HRSs (which results in building more and smaller HRSs), and, one could argue that a more spread-out refueling network would also be more convenient for drivers and make a more redundant system, if there are enough users. This is also supported by the findings in Fulton et al. [16]. Thus, while the optimization-based models give an interesting perspective on strategic locations to capture refueling demand with few HRSs, this model complements them with some interesting perspectives on how to structure the system in a longer term after the first vehicle introductions. Accommodating the large data volumes and the geospatial power detail possible in our model, together with financial factors, would make for an even stronger assessment.

The comparison with other studies points to the complexity of understanding future infrastructure requirements. Transport work is, in this study, extrapolated to 2050 by only correlating it with GDP. As shown in appendices A and B, this correlation is not strong for all countries. Additionally, basing the projections on modeled GDP introduces additional, inherited, uncertainties. Modeling future technical systems always include trade-offs of this kind, and the results should be used with this in mind.

Another assumption made in the SVENG model is that a flat share of trucks across all of Europe would run on hydrogen, which is a simplification. We have attempted to make this more accurate by only considering trucks going on long-haul routes longer than 360 km. In future developments, it might be interesting to create scenarios with diffusion rates differentiated between countries, and to include shorter range freight routes. Fulton et al. [16] simulates different scenarios for hydrogen road vehicle diffusion in California, and find that we could see high share of hydrogen technology in all studied modes. But, due to different conditions, notably policy [79–81], these results are not directly applicable to Europe, and more research in this area would facilitate better scenarios for hydrogen demand modeling. Furthermore, the connection to other mobile energy uses, like off-road, construction, shipping, and aviation, and stationary uses like industry and chemicals production, could further impact where it makes sense to locate refueling stations from a supply perspective. Future studies should integrate this to investigate the comprehensive transportation system.

According to results presented in this article, countries with high levels of long-haul road transport work will benefit from complying with AFIR, considering their simulated required additional refueling capacity between 2030 and 2050. However, for some countries, AFIR is more likely to entail a burdensome investment, unless hydrogen trucks assume a sizeable share of the total freight. The legislation is based on TEN-T road distance and number of urban nodes per country, which are easy and understandable metrics for legislators to work with. Evidently, this does not mean that they are parallel to the long-haul road transport work, and subsequent fuel demand, in a country. As discussed above, it is very uncertain where and to what extent hydrogen technology for transport might be adopted, and we have in this study only tested different outcomes by varying total market diffusion.

It is, furthermore, debatable whether the countries with low projected annual transport work will be the frontrunners in adopting hydrogen vehicles, which might further increase the gap between the installed infrastructure and the need. The recent, rapid, development of battery-electric trucks has additionally raised the question whether hydrogen trucks will be used at all, beyond niche applications [82]. Under-adoption in one or more countries could result in a situation where some EU countries would rather pay a fine than put money and effort into building unused HRSs. However, compliance with AFIR is meant to facilitate hydrogen truck diffusion, and investing early could be what is needed to spur adoption. Policymakers, fleet owners, and industries need to reflect on whether hydrogen is the right solution everywhere, and if so, how to ascertain a viable and self-sustaining hydrogen economy, with appropriate demand to match the supply.

In conclusion, SVENG incorporates higher detail on truck power requirements than previous models, which is found to increase the accuracy of the simulated future need for hydrogen refueling capacity in Europe. By including 597,000 cargo flows, the SVENG model provides a more comprehensive assessment over a larger area than previous articles studying hydrogen refueling infrastructure. Data from SVENG can, further, be used in the planning of the European energy infrastructure, and the model itself can be further extended to assess other drivetrains and transport modes.

CRediT authorship contribution statement

Joel Löfving: Writing – review & editing, Writing – original draft, Visualization, Validation, Software, Methodology, Investigation, Formal analysis, Data curation, Conceptualization. **Selma Brynolf:** Writing – review & editing, Supervision, Project administration, Funding acquisition, Conceptualization. **Maria Grahn:** Writing – review & editing, Supervision, Funding acquisition.

Funding

This work was supported by the competence center TechForH_2, which is hosted by Chalmers University of Technology and is financially supported by the Swedish Energy Agency (P2021-90268) and the member companies Volvo Group, Scania, Siemens Energy, GKN Aerospace, Powercell, Oxeon, RISE, Stena Rederier, Johnson Matthey and Insplorion.

Declaration of competing interest

The authors declare that they have no known competing financial interests or personal relationships that could have appeared to influence the work reported in this paper.

Acknowledgements

The authors want to extend their gratitude to Christian Boβer, for input on truck power modeling; Wasim Shoman, for explaining and introducing their model and the underlying data; Camille Megy and Negar Namazifard, for their comments on an early draft of the article.

Appendix. Supplementary data

Supplementary data to this article can be found online at https://doi.org/10.1016/j.ijhydene.2025.04.257.

References

[1] European Union. REGULATION OF THE EUROPEAN PARLIAMENT AND OF THE COUNCIL amending Regulation (EU) 2019/1242 as regards strengthening the CO2 emission performance standards for new heavy-duty vehicles and integrating reporting obligations, amending Regulation (EU) 2018/858 and repealing Regulation (EU) 2018/956. Brussels. https://data.consilium.europa.eu/doc/document/PE-29-2024-INIT/en/pdf; 2024.
[2] Li S, Djilali N, Rosen MA, Crawford C, Sui PC. Transition of heavy-duty trucks from diesel to hydrogen fuel cells: opportunities, challenges, and recommendations. Int J Energy Res 2022;46:11718–29. https://doi.org/10.1002/er.8066.
[3] Fulton LM, Ogden J. Sustainable transportation energy pathways. Transport Res Transport Environ 2021;91. https://doi.org/10.1016/j.trd.2020.102683.
[4] Lee DY, Elgowainy A, Kotz A, Vijayagopal R, Marcinkoski J. Life-cycle implications of hydrogen fuel cell electric vehicle technology for medium- and heavy-duty trucks. J Power Sources 2018;393:217–29. https://doi.org/10.1016/j.jpowsour.2018.05.012.
[5] DoE. Fuel cell electric vehicles. Alternative Fuels Data Center 2024. Accessed on: 07 Feb 2024, https://afdc.energy.gov/vehicles/fuel_cell.html.
[6] Zhang T, Qadrdan M, Wu J, Couraud B, Stringer M, Walker S, et al. A systematic review of modelling methods for studying the integration of hydrogen into energy systems. Renew Sustain Energy Rev 2025;208. https://doi.org/10.1016/j.rser.2024.114964.
[7] Çabukoglu E, Georges G, Küng L, Pareschi G, Boulouchos K. Fuel cell electric vehicles: an option to decarbonize heavy-duty transport? Results from a Swiss case-study. Transport Res Transport Environ 2019;70:35–48. https://doi.org/10.1016/j.trd.2019.03.004.
[8] Ragon P-L, Mulholland E, Basma H, Rodríguez F. A review of the AFIR proposal: public infrastructure needs to support the transition to a zero-emission truck fleet in the European Union. Accessed on: 14 March 2024, https://theicct.org/publication/afir-eu-hdv-infrastructure-mar22/; 2022.
[9] Halder P, Babaie M, Salek F, Haque N, Savage R, Stevanovic S, et al. Advancements in hydrogen production, storage, distribution and refuelling for a sustainable transport sector: hydrogen fuel cell vehicles. Int J Hydrogen Energy 2024;52: 973–1004. https://doi.org/10.1016/j.ijhydene.2023.07.204.
[10] Küffner C. Multi-level perspective for the development and diffusion of fuel cell heavy-duty trucks. Transport Res Transport Environ 2022;111. https://doi.org/10.1016/j.trd.2022.103460.
[11] Anderhofstadt B, Spinler S. Factors affecting the purchasing decision and operation of alternative fuel-powered heavy-duty trucks in Germany – a Delphi study. Transport Res Transport Environ 2019;73:87–107. https://doi.org/10.1016/j.trd.2019.06.003.
[12] Cullen DA, Neyerlin KC, Ahluwalia RK, Mukundan R, More KL, Borup RL, et al. New roads and challenges for fuel cells in heavy-duty transportation. Nat Energy 2021;6:462–74. https://doi.org/10.1038/s41560-021-00775-z.
[13] Bae Y, Rindt CR, Mitra SK, Ritchie SG. Fleet operator perspectives on alternative fuels for heavy-duty vehicles. Transp Policy 2024;149:36–48. https://doi.org/10.1016/j.tranpol.2024.01.023.
[14] Trencher G, Wesseling J. Roadblocks to fuel-cell electric vehicle diffusion: evidence from Germany, Japan and California. Transport Res Transport Environ 2022;112. https://doi.org/10.1016/j.trd.2022.103458.
[15] Hardman S, Steinberger-Wilckens R. Mobile phone infrastructure development: lessons for the development of a hydrogen infrastructure. Int J Hydrogen Energy 2014;16:8185–93. https://www.scopus.com/inward/record.uri?eid=2-s2.0-84900389735&doi=10.1016%2fj.ijhydene.2014.03.156&partnerID=40&md5=009958e003af1f442f46c06c503beeea.
[16] Fulton L, Jenn A, Yang C, Burke A, Acharya TD, Li X, et al. California hydrogen analysis Project: the future role of hydrogen in a carbon-neutral California: final synthesis modeling report. Accessed on: 15 March 2024, https://escholarship.org/uc/item/27m7g841; 2023.
[17] ITF. How governments can bring low-emission trucks to our roads – and fast. Accessed on: 2 March 2024, https://www.itf-oecd.org/sites/default/files/docs/low-emission-trucks.pdf; 2023.
[18] Greene DL, Ogden JM, Lin Z. Challenges in the designing, planning and deployment of hydrogen refueling infrastructure for fuel cell electric vehicles. eTransportation 2020;6. https://doi.org/10.1016/j.etran.2020.100086.
[19] Torkayesh AE, Venghaus S. Decoding the transport policy maze towards climate neutrality: cross-sectoral policy landscapes. Renew Sustain Energy Rev 2024;206. https://doi.org/10.1016/j.rser.2024.114865.
[20] European Union. Regulation (EU) 2023/1804 of the European Parliament and of the Council of 13 September 2023 on the deployment of alternative fuels infrastructure, and repealing Directive 2014/94/EU. Off J Eur Union 2023. https://eur-lex.europa.eu/legal-content/EN/TXT/?uri=uriserv%3AOJ.L_.2023.234.01.0001.01.ENG&toc=OJ%3AL%3A2023%3A234%3ATOC.
[21] Shirizadeh B, Ailleret A, Cartry C, Douguet S, Gehring T, Maden S, et al. Climate neutrality in European heavy-duty road transport: how to decarbonise trucks and buses in less than 30 years? Energy Convers Manag 2024;309. https://doi.org/10.1016/j.enconman.2024.118438.
[22] Ganter A, Gabrielli P, Sansavini G. Near-term infrastructure rollout and investment strategies for net-zero hydrogen supply chains. Renew Sustain Energy Rev 2024;194. https://doi.org/10.1016/j.rser.2024.114314.
[23] Aryanpur V, O'Gallachoir B, Dai H, Chen W, Glynn J. A review of spatial resolution and regionalisation in national-scale energy systems optimisation models. Energy Strategy Rev 2021;37. https://doi.org/10.1016/j.esr.2021.100702.
[24] Martínez-Gordón R, Morales-España G, Sijm J, Faaij APC. A review of the role of spatial resolution in energy systems modelling: lessons learned and applicability to the North Sea region. Renew Sustain Energy Rev 2021;141. https://doi.org/10.1016/j.rser.2021.110857.
[25] Ferrara A, Jakubek S, Hametner C. Energy management of heavy-duty fuel cell vehicles in real-world driving scenarios: robust design of strategies to maximize the hydrogen economy and system lifetime. Energy Convers Manag 2021;232. https://doi.org/10.1016/j.enconman.2020.113795.
[26] Lago Sari R, Fogue Robles A, Monsalve Serrano J, Cleary D. Techno-economic assessment of hydrogen as a fuel for internal combustion engines and proton exchange membrane fuel cells on long haul applications. Energy Convers Manag 2024;311. https://doi.org/10.1016/j.enconman.2024.118522.

[27] Riera JA, Lima RM, Knio OM. A review of hydrogen production and supply chain modeling and optimization. Int J Hydrogen Energy 2023;48:13731–55. https://doi.org/10.1016/j.ijhydene.2022.12.242.
[28] Speth D, Plötz P, Funke S, Vallarella E. Public fast charging infrastructure for battery electric trucks—a model-based network for Germany. Environ Res: Infrastructure and Sustainability 2022;2. https://doi.org/10.1088/2634-4505/ac6442.
[29] Hodgson MJ. A flow-capturing location-allocation model. Geogr Anal 1990;22: 270–9. https://doi.org/10.1111/j.1538-4632.1990.tb00210.x.
[30] Capar I, Kuby M. An efficient formulation of the flow refueling location model for alternative-fuel stations. IIE Trans 2012;44:622–36. https://doi.org/10.1080/0740817X.2011.635175.
[31] Capar I, Kuby M, Leon VJ, Tsai YJ. An arc cover-path-cover formulation and strategic analysis of alternative-fuel station locations. Eur J Oper Res 2013;227: 142–51. https://doi.org/10.1016/j.ejor.2012.11.033.
[32] Jochem P, Szimba E, Reuter-Oppermann M. How many fast-charging stations do we need along European highways? Transport Res Transport Environ 2019;73: 120–9. https://doi.org/10.1016/j.trd.2019.06.005.
[33] Rose P, Nugroho R, Gnann T, Plötz P, Wietschel M, Reuter-Oppermann M. Optimal development of alternative fuel station networks considering node capacity restrictions. Transport Res Transport Environ 2020;78. https://doi.org/10.1016/j.trd.2019.11.018.
[34] De Padova A, Schiera DS, Minuto FD, Lanzini A. Spatial MILP optimization framework for siting Hydrogen Refueling Stations in heavy-duty freight transport. Int J Hydrogen Energy 2024;94:669–86. https://doi.org/10.1016/j.ijhydene.2024.11.086.
[35] Liu N, Xie F, Lin Z, Jin M. Evaluating national hydrogen refueling infrastructure requirement and economic competitiveness of fuel cell electric long-haul trucks. Mitig Adapt Strategies Glob Change 2020;25:477–93. https://doi.org/10.1007/s11027-019-09896-z.
[36] Acharya TD, Jenn AT, Miller MR, Fulton LM. Spatial modeling of future light- and heavy-duty vehicle travel and refueling patterns in California. Accessed on: 15 March 2024, https://escholarship.org/uc/item/1mf9r7g1; 2021.
[37] Reuter-Oppermann M, Funke S, Jochem P, Graf F. How many fast charging stations do we need along the German highway network? Electric Vehicle Symposium 2017;30(EVS30). Stuttgart, Germany, https://www.researchgate.net/publication/320550413_How_Many_Fast_Charging_Stations_Do_We_Need_Along_the_German_Highway_Network.
[38] Maestre VM, Ortiz A, Ortiz I. Decarbonizing the Spanish transportation sector by 2050: design and techno-economic assessment of the hydrogen generation and supply chain. Int J Hydrogen Energy 2023;48:39514–30. https://doi.org/10.1016/j.ijhydene.2023.05.154.
[39] Guzzini A, Brunaccini G, Aloisio D, Pellegrini M, Saccani C, Sergi F. A new geographic information system (GIS) tool for hydrogen value chain planning optimization: application to Italian highways. Sustainability 2023;15. https://doi.org/10.3390/su15032080.
[40] Kim H, Eom M, Kim BI. Development of strategic hydrogen refueling station deployment plan for Korea. Int J Hydrogen Energy 2020;45:19900–11. https://doi.org/10.1016/j.ijhydene.2020.04.246.
[41] He C, Sun H, Xu Y, Lv S. Hydrogen refueling station siting of expressway based on the optimization of hydrogen life cycle cost. Int J Hydrogen Energy 2017;42: 16313–24. https://doi.org/10.1016/j.ijhydene.2017.05.073.
[42] Cutore E, Fichera A, Inturri G, Le Pira M, Volpe R. Spatially-explicit optimization of an integrated wind-hydrogen supply chain network for the transport sector: the case study of Sicily. Int J Hydrogen Energy 2024;52:761–74. https://doi.org/10.1016/j.ijhydene.2023.10.105.
[43] Zhou J, Du P, Liang G, Chang H, Liu S. Hydrogen station location optimization coupling hydrogen sources and transportation along the expressway. Int J Hydrogen Energy 2024;54:1094–109. https://doi.org/10.1016/j.ijhydene.2023.11.284.
[44] Kuvvetli Y. Multi-objective and multi-period hydrogen refueling station location problem. Int J Hydrogen Energy 2020;45:30845–58. https://doi.org/10.1016/j.ijhydene.2020.08.126.
[45] Zhou Y, Qin X, Mei W, Yang W, Ni M. Multi-period urban hydrogen refueling stations site selection and capacity planning with many-objective optimization for hydrogen supply chain. Int J Hydrogen Energy 2024;79:1427–41. https://doi.org/10.1016/j.ijhydene.2024.07.067.
[46] Shoman W, Yeh S, Sprei F, Plötz P, Speth D. Battery electric long-haul trucks in Europe: public charging, energy, and power requirements. Transport Res Transport Environ 2023;121. https://doi.org/10.1016/j.trd.2023.103825.
[47] Speth D, Sauter V, Plötz P, Signer T. Synthetic European road freight transport flow data. Data Brief 2022;40. https://doi.org/10.1016/j.dib.2021.107786.
[48] Martineau R. Fast flow future for heavy-duty hydrogen trucks. https://www.nrel.gov/news/program/2022/fast-flow-future-heavy-duty-hydrogen-trucks.html; 2022.
[49] Pihlatie M, Ranta M, Rahkola P, Åman R. Zero-emission truck powertrains for regional and long-haul missions. World Electric Vehicle Journal 2023;14. https://doi.org/10.3390/wevj14090253.
[50] Danebergs J. Techno-economic study of hydrogen as a heavy-duty truck fuel: a case study on the transport corridor oslo. Trondheim: KTH; 2019.
[51] Eurostat. NUTS - Nomenclature for Territorial Units for Statistics. https://ec.europa.eu/eurostat/web/nuts/overview.
[52] Tarvydas D. The role of hydrogen in energy decarbonisation scenarios – views on 2030 and 2050. Luxembourg 2022. Accessed on: 1 April 2024, https://publications.jrc.ec.europa.eu/repository/bitstream/JRC131299/JRC131299_01.pdf.
[53] World Bank. GDP, PPP (current international $)(NY.GDP. MKTP.PP.CD) 2023.
[54] Eurostat. National road transport by type of goods and type of transport (t, tkm) - annual data (from 2008 onwards). https://ec.europa.eu/eurostat/databrowser/view/road_go_na_tgtt_custom_8139003/default/table; 2023.
[55] Eurostat. Road cabotage transport of reporting country by country in which cabotage takes place (t, tkm) - (from 1999 onwards). https://ec.europa.eu/eurostat/databrowser/view/road_go_ca_hac_custom_8138989/default/table; 2023.
[56] Eurostat. International road freight transport - loaded goods in reporting country by country of unloading, type of goods and type of transport (t) - annual data (from 2008 onwards). https://ec.europa.eu/eurostat/databrowser/view/road_go_ia_lgtt_custom_8138965/default/table; 2023.
[57] IIASA. GDP 2023 2024. https://data.ece.iiasa.ac.at/ssp.
[58] Crespo Cuaresma J. Income projections for climate change research: a framework based on human capital dynamics. Glob Environ Change 2017;42:226–36. https://doi.org/10.1016/j.gloenvcha.2015.02.012.
[59] Szimba E, Kraft M, Ihrig J, Schimke A, Schnell O, Kawabata Y, et al. ETISplus database content and methodology: ETISplus deliverable D6. 2013.
[60] European Commission. REPORT FROM THE COMMISSION under Regulation (EU) 2018/956 analysing the data transmitted by Member States and manufacturers for the reporting period 2020 on CO2 emissions from and fuel consumption of new heavy-duty vehicles Brussels. Accessed on: 1 June 2024, https://eur-lex.europa.eu/legal-content/EN/TXT/PDF/?uri=CELEX:52023DC0517; 2023.
[61] Eurostat. Empty road journeys by type of operation, 2018 (% share in vehicle-kilometres). Accessed on: 01 April 2024, https://ec.europa.eu/eurostat/statistics-explained/index.php?title=File:Empty_road_journeys_by_type_of_operation,_2018_(%25_share_in_vehicle-kilometres).png; 2018.
[62] European Space Agency. Copernicus DEM - global and European digital elevation model (COP-dem). https://ec.europa.eu/eurostat/web/gisco/geodata/reference-data/elevation/copernicus-dem/elevation; 2023.
[63] Zhang C, Kotz A, Kelly K, Rippelmeyer L. Development of heavy-duty vehicle representative driving cycles via decision tree regression. Transport Res Transport Environ 2021;95. https://doi.org/10.1016/j.trd.2021.102843.
[64] European Commission. Support Preparation of Legislation on Trailers Certification, Task 2: development of a detailed methodology and procedure for the determination of the effect of trailers and semi-trailers bodyworks with regards to the CO2 emissions/fuel consumption of the towing vehicle. Accessed on: 25 May 2024, https://climate.ec.europa.eu/document/download/e9e49183-5acf-4dd4-a235-d17bea14d309_en?filename=policy_transport_road_co2_energy_efficiency_2_en.pdf; 2022.
[65] Delgado O, Rodriguez F, Muncrief R. Fuel efficiency technology in European heavy-duty vehicles: baseline and potential for the 2020–2030 time frame. Accessed on: https://theicct.org/sites/default/files/publications/EU-HDV-Tech-Potential_ICCT-white-paper_14072017_vF.pdf; 2017.
[66] European Commission. Working document for the methodology drafting for the CO2 monitoring of HD vehicles (draft). Accessed on, https://climate.ec.europa.eu/system/files/2017-03/technical_annex_en.pdf; 2014.
[67] Song Z, Pan Y, Chen H, Zhang T. Effects of temperature on the performance of fuel cell hybrid electric vehicles: a review. Appl Energy 2021;302:117572. https://doi.org/10.1016/j.apenergy.2021.117572.
[68] European Union. Road rules and safety. https://europa.eu/youreurope/citizens/travel/driving-abroad/road-rules-and-safety/index_en.htm; 2023.
[69] Truck Daimler. Fuel-cell technology: daimler truck builds first mercedes-benz GenH2 truck customer-trial fleet. Accessed on: 17 April 2024, https://www.daimlertruck.com/en/newsroom/pressrelease/fuel-cell-technology-daimler-truck-builds-first-mercedes-benz-genh2-truck-customer-trial-fleet-52552943; 2023.
[70] Doppler C, Lindner-Rabl B. Fuel cell trucks: thermal challenges in heat exchanger layout. Energies 2023;16. https://doi.org/10.3390/en16104024.
[71] Basma H, Rodríguez F. Fuel cell electric tractor-trailers: technology overview and fuel economy 2022. https://theicct.org/publication/fuel-cell-tractor-trailer-tech-fuel-jul22/. [Accessed 1 April 2024].
[72] Ahluwalia RK, Roh HS, Peng JK, Papadias D, Baird AR, Hecht ES, et al. Liquid hydrogen storage system for heavy duty trucks: configuration, performance, cost, and safety. Int J Hydrogen Energy 2023;48:13308–23. https://doi.org/10.1016/j.ijhydene.2022.12.152.
[73] Link S, Plötz P. Geospatial truck parking locations data for Europe. Data Brief 2024;54. https://doi.org/10.1016/j.dib.2024.110277.
[74] Eurostat. Eurostat census grid 2021. https://ec.europa.eu/eurostat/web/gisco/geodata/reference-data/population-distribution-demography/geostat; 2021.
[75] Reis S, Liska T, Steinle S, Carnell E, Leaver D, Roberts E, et al. UK gridded population 2011 based on census 2011 and land cover map 2015. https://www.data.gov.uk/dataset/ca2daae8-8f36-4279-b15d-78b0463c61db/uk-gridded-population-2011-based-on-census-2011-and-land-cover-map-2015#licence-info; 2017.
[76] Fuse M, Noguchi H, Seya H. Near-term location planning of hydrogen refueling stations in Yokohama City. Int J Hydrogen Energy 2021;46:12272–9. https://doi.org/10.1016/j.ijhydene.2020.09.199.
[77] Elgowainy A, Reddi K. Hydrogen refueling analysis of heavy-duty fuel cell vehicle fleet. 2017 DOE hydrogen and fuel cells program. 2018. https://www.hydrogen.energy.gov/docs/hydrogenprogramlibraries/pdfs/review17/pd014_elgowainy_2017_o.pdf. [Accessed 1 April 2024].
[78] Hoffman B. Hydrogen in the alternative infrastructure regulation (AFIR) – incl. Actions taken in Germany. Hydrogen for clean transport 2023 – hydrogen mobility Europe Project final conference. 2023. Rotterdam, https://h2me.eu/wp-content/uploads/2023/06/2023-0508_G25-Hoffmann-HRS-AFIR-Hydrogen-Mobility-Europe-Conference_2023-0510_viewer.pdf.

[79] CARB. Advanced clean fleets 2024. https://ww2.arb.ca.gov/our-work/programs/advanced-clean-fleets. [Accessed 3 March 2024].
[80] CARB. Advanced clean trucks 2024. https://ww2.arb.ca.gov/our-work/programs/advanced-clean-trucks. [Accessed 3 March 2024].
[81] California HVIP. Hybrid and zero-emission truck and BUS voucher incentive project. https://californiahvip.org/. [Accessed 3 March 2024].
[82] Plötz P. Hydrogen technology is unlikely to play a major role in sustainable road transport. Nature Electronics 2022;5:8–10. https://doi.org/10.1038/s41928-021-00706-6.